Dispersion tailoring of the quarter-wave Bragg reflection waveguide

Brian R. West and A. S. Helmy

Edward S. Rogers Sr. Department of Electrical and Computer Engineering, University of Toronto
10 King's College Rd., Toronto, ON, Canada M5S 3G4
a.helmy@utoronto.ca

Abstract: We present analytical formulae for the polarization dependent first- and second-order dispersion of a quarter-wave Bragg reflection waveguide (QtW-BRW). Using these formulae, we develop several qualitative properties of the QtW-BRW. In particular, we show that the birefringence of these waveguides changes sign at the QtW wavelength. Regimes of total dispersion corresponding to predominantly material-dominated and waveguide-dominated dispersion are identified. Using this concept, it is shown that the QtW-BRW can be designed so as to provide anomalous group velocity dispersion of large magnitude, or very small GVD of either sign, simply by an appropriate chose of layer thicknesses. Implications on nonlinear optical devices in compound semiconductors are discussed.

OCIS codes: (230.7370) Waveguides; (230.1480) Bragg reflectors; (130.3120) Integrated optics devices

References and links

1. A. S. Helmy and B. R. West, "Phase matching using Bragg reflector waveguides," in *Proceedings of 18th Annual Meeting of the IEEE Lasers and Electro-Optics Society* (Institute of Electrical and Electronics Engineers, Sydney, 2005), pp. 424-425.
2. A. S. Helmy, "Phase matching using Bragg reflection waveguides for monolithic nonlinear optics applications," Opt. Express **14**, 1243-1252 (2006) http://www.opticsexpress.org/abstract.cfm?URI=OPEX-14-3-1243.
3. Y. Sakurai and F. Koyama, "Proposal of tunable hollow waveguide distributed Bragg reflectors," Jap. J. Appl. Phys. **43,** L631-L633 (2004).
4. E. Simova and I. Golub, "Polarization splitter/combiner in high index contrast Bragg reflector waveguides," Opt. Express **11**, 3425-3430 (2003), http://www.opticsexpress.org/abstract.cfm?URI=OPEX-11-25-3425.
5. A. Mizrahi and L. Schächter, "Optical Bragg accelerators," Phys. Rev. E. **70**, Art. 016505(2) (2004).
6. S. Nakamura, K. Tajima, "Analysis of subpicosecond full-switching with a symmetric Mach-Zehnder all-optical switch," Jap. J. Appl. Phys. **35**, L1426-L1429 (1996).
7. K. Cheng, ed., *Handbook of Optical Components and Engineering* (Wiley Interscience, 2003).
8. G. P. Agrawal, *Nonlinear Fiber Optics* (Academic Press, 1989).
9. U. Peschel, T. Peschel, and F. Lederer, "A compact device for highly efficient dispersion compensation in fiber transmission," Appl. Phys. Lett. **67**, 2111-2113 (1995).
10. Y. Lee, A. Takei, T. Taniguchi, and H. Uchiyama, "Temperature tuning of dispersion compensation using semiconductor asymmetric coupled waveguides," J. Appl. Phys. **98**, 113102 (2005).
11. M. A. Foster, A. L. Gaeta, Q. Cao, and R. Trebino, "Soliton-effect compression of supercontinuum to few-cycle durations in photonic nanowires," Opt. Express **13**, 6848-6855 (2005), http://www.opticsexpress.org/abstract.cfm?URI=OPEX-13-18-6848.
12. E. Valentinuzzi, "Dispersive properties of Kerr-like nonlinear optical structures," J. Lightwave Technol. **16**, 152-155 (1998).
13. G. Bouwmans, L. Bigot, Y. Quiquempois, F. Lopez, L. Provino, and M. Douay, "Fabrication and characterization of an all-solid 2D photonic bandgap fiber with a low-loss region (< 20 dB/km) around 1550 nm," Opt. Express **13**, 8452-8459 (2005), http://www.opticsexpress.org/abstract.cfm?URI=OPEX-13-21-8452.

#68524 - $15.00 USD Received 27 February 2006; revised 17 April 2006; accepted 18 April 2006

14. T. D. Engeness, M. Ibanescu, S. G. Johnson, O. Weisberg, M. Skorobogatiy, S. Jacobs, and Y. Fink, "Dispersion tailoring and compensation by modal interactions in OmniGuide fibers," Opt. Express **11**, 1175-1196 (2003), http://www.opticsexpress.org/abstract.cfm?URI=OPEX-11-10-1175.
15. A. Mizrahi and L. Schächter, "Bragg reflection waveguides with a matching layer," Opt. Express **12**, 3156-3170 (2004), http://www.opticsexpress.org/abstract.cfm?URI=OPEX-12-14-3156.
16. I. V. Shadrivov, A. A. Sukhorukov, Y. S. Kivshar, A. A. Zharov, A. D. Boardman, and P. Egan, "Nonlinear surface waves in left-handed materials," Phys. Rev. E **69**, 016617 (2004).
17. Y. Sakurai and F. Koyama, "Control of group delay and chromatic dispersion in tunable hollow waveguide with highly reflective mirrors," Jap. J. Appl. Phys. **43,** 5828-5311 (2004).
18. P. Yeh and A. Yariv, "Bragg reflection waveguides," Opt. Commun. **19**, 427-430 (1976).
19. P. Yeh, A. Yariv, and C.-S. Hong, "Electromagnetic propagation in periodic stratified media: I. General theory," J. Opt. Soc. Am. **67**, 428-438 (1977).
20. B. R. West and A. S. Helmy, "Properties of the quarter-wave Bragg reflection waveguide: Theory," J. Opt. Soc. Am. B (to be published).
21. A. S. Deif, *Advanced Matrix Theory for Scientists and Engineers* (Routledge, 1987).
22. S. Adachi, "GaAs, AlAs, and $Al_xGa_{1-x}As$ material parameters for use in research and device applications," J. Appl. Phys. **58**, R1-R29 (1985).
23. M. A. Afromowitz, "Refractive index of $Ga_{1-x}Al_xAs$," Solid State Commun. **15**, 59-63 (1974).
24. A. N. Pikhtin and A. D. Yas'kov, "Dispersion of refractive-index of semiconductors with diamond and zincblende structures," Sov. Phys. Semicond. **12**, 622-626 (1978).
25. S. Gehrsitz, F. K. Reinhart, C. Gourgon, N. Herres, A. Vonlanthen, and H. Sigg, "The refractive index of $Al_xGa_{1-x}As$ below the band gap: Accurate determination and empirical modeling," J Appl. Phys. **87**, 7825-7837 (2000).
26. T. C. Kleckner, A. S. Helmy, K. Zeaiter, D. C. Hutchings, and J. S. Aitchison, "Dispersion and modulation of the linear optical properties of GaAs-AlAs superlattice waveguides using quantum-well intermixing," IEEE J. Quantum Electron. **42**, 280-286 (2006).
27. B. R. West and A. S. Helmy, "Analysis and design equations for phase matching using Bragg reflector waveguides," IEEE J. Sel. Top. Quantum Electron. (to be published).

1. Introduction

The Bragg reflection waveguide (BRW) is a structure in which waveguiding is achieved by distributed reflection within a periodic cladding, as opposed to total internal reflection. By utilizing Bragg reflection, it is possible for the waveguide core to have a lower index than the cladding, which is beneficial for gas- or liquid-core waveguiding. In fact, the guided modes may have effective indices lower than all material indices, provided that the transverse propagation vector lies within the Bragg stop-band of the cladding. Numerous other benefits are afforded by BRWs due to this unique guiding mechanism. These waveguides have recently received interest for applications such as phase matching for nonlinear frequency conversion [1, 2], mechanically tunable air-core filters [3], polarization splitters [4], and electron accelerators [5]. However, one other application in which BRWs can be extremely useful is the control of overall waveguide dispersion. This feature is of paramount importance for devices which use or manipulate optical pulses in picosecond and femtosecond regimes in materials with nonlinearities and/or considerable dispersion coefficients in the operating wavelength range. One popular example is semiconductors at a wavelength of operation near their bandgap.

Semiconductors provide useful functionality such as amplification, modulation and nonlinear effects when operated near the material resonances such as the bandgap. In these regimes, the material dispersion is dominant over all other types of dispersion including waveguide dispersion. This produces a limitation on the useful device length due to temporal pulse walk-off and pulse broadening [6]. These obstacles effectively set a lower limit on the useful pulse widths which can be used for a given device length. However, device functionality and figures of merit such as amplification factor or modulation depth often rely on the length of the device [7], so a tradeoff in design principles clearly arises. Additionally, in some devices which utilize nonlinear effects – for example, devices which rely on temporal soliton or soliton-like pulse propagation such as switches, pulse shaping elements or short

#68524 - $15.00 USD Received 27 February 2006; revised 17 April 2006; accepted 18 April 2006

pulse mode-locked laser sources – the dispersion defines the threshold intensity at which solitons can be formed [8]. Therefore, by tuning the dispersion parameters in the waveguides forming these devices, control over the temporal soliton threshold power can be achieved. Moreover, because the dispersion sign can also be reversed, BRWs can be used to compel the propagating mode to possess a dispersion sign opposite to that of their constituent materials. By doing so, BRWs may enable the propagation of bright and dark temporal solitons in self-focusing materials [8], an attractive feature for many nonlinear photonic devices which has not been easily attainable to date.

While the control of waveguide dispersion have been often reported in propagation orthogonal to periodic gratings, these structures have some limitation due to the tradeoff between the dispersion obtained and the structural scattering losses. Numerous attempts to design practical structures with no periodic perturbation of the optical properties that provide the capability of tuning the dispersion have been reported [9, 10]. Pulse compression in photonic nano-wires [11], limited tuning of the waveguide dispersion in depressed cladding waveguides [12], fibers with photonic bandgap claddings [13, 14], Bragg waveguides with additional matching layers [15] and nonlinear surface waves at the interface of left- and right-handed media [16] were all reported previously. Some challenges that face the structures reported to date include the losses in the propagation direction due to structural scattering, the amount of control over the dispersion magnitude with respect to the material dispersion, and the inability to reverse the sign of dispersion.

In this work, we demonstrate how the second-order dispersion of BRWs can be tuned and reversed in sign using BRWs. This control will result in propagating modes with a total dispersion, comprised of material dispersion as well as waveguide dispersion, that is set by the BRW design parameters. To demonstrate these effects we use a rigorous perturbation approach to derive analytical formulae for the first- and second-order polarization dependent dispersion of a nominally quarter-wave Bragg reflection waveguide (QtW-BRW). The motivation to take this approach rather than the numerical ray-optics approach in [17] to demonstrate the dispersion tuning capabilities of BRWs is two-fold. First, analytical solutions elucidate the relation between waveguide design parameters and dispersion, thus facilitating the design of waveguides with desired dispersive properties. From a more practical standpoint, calculating higher orders of dispersion from the modeled dispersion curve through numerical differentiation or curve fitting may be inaccurate for some BRW designs due to poor conditioning of the modeled data (e.g. for very large or very small magnitudes of dispersion). In section 2, the QtW-BRW will be described, and dispersion formulae are derived in section 3 and compared with numerical solutions for a representative QtW-BRW. Section 4 contains a discussion of the relative contributions of waveguide and material dispersion, and it is shown that for a wide range of waveguide designs, precise knowledge of the material dispersion is not required for accurate calculation of the waveguide dispersion. We introduce the concept of a normalized effective index and show that this value is critically related to the dispersion in a QtW-BRW, and discuss the implications of this work on improving nonlinear device performance in semiconductors.

2. The quarter-wave Bragg reflection waveguide

A one-dimensional Bragg reflection waveguide, first analyzed in detail by Yeh and co-workers [18, 19], is shown in Fig. 1. The cladding consists of slabs of index n_1 and n_2, with thickness a and b, respectively, where $n_1 > n_2$. The cladding period is denoted as $\Lambda = a + b$. The core has index n_{co} and thickness t_{co}. For this analysis it is assumed that the cladding consists of an infinite number of periods, although the results are valid for structures with a reasonably large number of periods [20]. In addition, it is assumed that the waveguide is symmetric about the core. This is not a requirement of BRWs, but calculation of dispersion becomes considerably more complex in the presence of waveguide asymmetry. Hence we shall consider symmetric waveguides here for simplicity, although the methodology is applicable to asymmetric structures as well.

The transverse propagation vector takes on discrete values in each slab,

#68524 - $15.00 USD Received 27 February 2006; revised 17 April 2006; accepted 18 April 2006

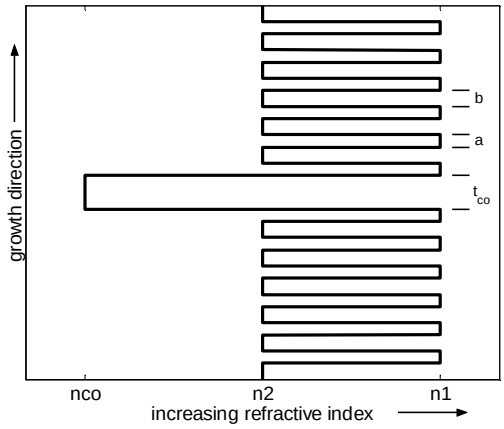

Fig. 1. Refractive index profile of a BRW.

$$k_i = \frac{\omega}{c}\sqrt{n_i^2 - n_{\text{eff}}^2} \tag{1}$$

(i = 1, 2, co), where ω is the angular frequency of the guided radiation and c is the speed of light. The guided modes are determined by a mode dispersion equation, derived in [20] using a field transfer matrix description of the periodic cladding:

$$\begin{aligned}
&\frac{1}{k_{\text{co}}}\cot\left(\frac{k_{\text{co}}t_{\text{co}}}{2}\right) = \frac{-i}{k_1}\frac{e^{iK_{\text{TE}}\Lambda} - A_{\text{TE}} + B_{\text{TE}}}{e^{iK_{\text{TE}}\Lambda} - A_{\text{TE}} - B_{\text{TE}}}, && \text{(TE)}\\
&\frac{1}{k_{\text{co}}}\cot\left(\frac{k_{\text{co}}t_{\text{co}}}{2}\right) = \frac{-i}{k_1}\left(\frac{n_1}{n_{\text{co}}}\right)^2\frac{e^{iK_{\text{TM}}\Lambda} - A_{\text{TM}} + B_{\text{TM}}}{e^{iK_{\text{TM}}\Lambda} - A_{\text{TM}} - B_{\text{TM}}}, && \text{(TM, } n_1^2k_2 < n_2^2k_1\text{)}\\
&k_{\text{co}}\cot\left(\frac{k_{\text{co}}t_{\text{co}}}{2}\right) = ik_1\left(\frac{n_{\text{co}}}{n_1}\right)^2\frac{e^{iK_{\text{TM}}\Lambda} - A_{\text{TM}} - B_{\text{TM}}}{e^{iK_{\text{TM}}\Lambda} - A_{\text{TM}} + B_{\text{TM}}}, && \text{(TM, } n_1^2k_2 > n_2^2k_1\text{)}
\end{aligned} \tag{2}$$

with matrix elements

$$\begin{aligned}
A_{\text{TE}} &= e^{ik_1a}\left[\cos k_2b + \frac{i}{2}\left(\frac{k_2}{k_1} + \frac{k_1}{k_2}\right)\sin k_2b\right]\\
A_{\text{TM}} &= e^{ik_1a}\left[\cos k_2b + \frac{i}{2}\left(\frac{n_2^2k_1}{n_1^2k_2} + \frac{n_1^2k_2}{n_2^2k_1}\right)\sin k_2b\right]\\
B_{\text{TE}} &= e^{-ik_1a}\left[\frac{i}{2}\left(\frac{k_2}{k_1} - \frac{k_1}{k_2}\right)\sin k_2b\right]\\
B_{\text{TM}} &= e^{-ik_1a}\left[\frac{i}{2}\left(\frac{n_2^2k_1}{n_1^2k_2} - \frac{n_1^2k_2}{n_2^2k_1}\right)\sin k_2b\right].
\end{aligned} \tag{3}$$

The term $\exp(iK_{\text{TE(TM)}}\Lambda)$ is the one physically realizable eigenvalue of the field transfer matrix

#68524 - $15.00 USD Received 27 February 2006; revised 17 April 2006; accepted 18 April 2006

$$M_{\mathrm{TE(TM)}}^{\mathrm{FT}} = \begin{bmatrix} A_{\mathrm{TE(TM)}} & B_{\mathrm{TE(TM)}} \\ B_{\mathrm{TE(TM)}}^{*} & A_{\mathrm{TE(TM)}}^{*} \end{bmatrix} \tag{4}$$

which, due to the unimodularity of M^{FT}, can be expressed as

$$K_{\mathrm{TE(TM)}}\Lambda = \cos^{-1}[\mathrm{Re}(A_{\mathrm{TE(TM)}})]. \tag{5}$$

The two regimes of TM waveguiding described in Eq. (2) are separated by the external Brewster angle condition in the cladding, at which energy localization is lost. We define here a TM symmetry factor

$$\rho \equiv \frac{n_1^2 k_2}{n_2^2 k_1} \tag{6}$$

and for the remainder of this paper we will refer to the "even" ($\rho < 1$) and "odd" ($\rho > 1$) TM modes in reference to their symmetry, as discussed in [20].

The quarter-wave BRW (QtW-BRW) is one in which each cladding layer has an optical thickness of $\lambda/4$ with respect to the transverse propagation vector:

$$k_1 a = k_2 b = \frac{\pi}{2}. \tag{7}$$

This places the k_i in the middle of the stop-band, ensuring strong reflection and hence optimal confinement in the core. As derived in [20], the effective index in this case is independent of polarization for slab waveguides and is equal to

$$n_{\mathrm{eff}} = \sqrt{n_{\mathrm{co}}^2 - \left(\frac{\pi c}{\omega_0 t_{\mathrm{co}}}\right)^2} \tag{8}$$

for the fundamental mode, where the subscript on ω_0 signifies the nominal angular frequency at which the quarter-wave condition is satisfied, as opposed to the variable ω that will be used later in this paper. In addition, the matrix elements and eigenvalue reduce to

$$\begin{aligned} A_{\mathrm{TE}} &= -\frac{1}{2}\left(\frac{k_2}{k_1} + \frac{k_1}{k_2}\right) \quad B_{\mathrm{TE}} = \frac{1}{2}\left(\frac{k_2}{k_1} - \frac{k_1}{k_2}\right) \\ A_{\mathrm{TM}} &= -\frac{1}{2}\left(\frac{1}{\rho} + \rho\right) \quad B_{\mathrm{TM}} = \frac{1}{2}\left(\frac{1}{\rho} - \rho\right) \\ e^{iK_{\mathrm{TE}}\Lambda} &= -\left(\frac{k_2}{k_1}\right) \qquad e^{iK_{\mathrm{TM}}\Lambda} = \begin{cases} -\rho & \text{EVEN} \\ -\dfrac{1}{\rho} & \text{ODD}. \end{cases} \end{aligned} \tag{9}$$

#68524 - $15.00 USD Received 27 February 2006; revised 17 April 2006; accepted 18 April 2006

3. Analytical determination of dispersion

To calculate the dispersion of a nominally quarter-wave BRW, we add a perturbation term Δk_i to each transverse propagation vector and examine the resulting change in Eq. (2). As the polarization degeneracy is lifted when the waveguide is detuned from the quarter-wave condition, the k_i become polarization dependent by Eq. (1). Polarization subscripts on the k_i will be omitted for brevity; however, those on the matrix elements will remain in order to indicate that their defining equations are unique to a specific polarization, as shown in Eq. (3).

Using Eq. (2), the perturbed TE mode dispersion equation is given by

$$\frac{1}{k_{co}+\Delta k_{co}}\cot\left(\frac{(k_{co}+\Delta k_{co})t_{co}}{2}\right) = \frac{-i}{k_1+\Delta k_1}\left(\frac{[e^{iK_{TE}\Lambda}+\Delta(e^{iK_{TE}\Lambda})]-[A_{TE}+\Delta A_{TE}]+[B_{TE}+\Delta B_{TE}]}{[e^{iK_{TE}\Lambda}+\Delta(e^{iK_{TE}\Lambda})]-[A_{TE}+\Delta A_{TE}]-[B_{TE}+\Delta B_{TE}]}\right). \quad (10)$$

Expanding Eq. (10) to first order in the perturbation terms,

$$\frac{-\Delta k_{co}t_{co}}{2k_{co}} \approx \frac{-i}{k_1}\left(\frac{\Delta(e^{iK_{TE}\Lambda})-\Delta A_{TE}+\Delta B_{TE}}{e^{iK_{TE}\Lambda}-A_{TE}-B_{TE}}\right) \quad (11)$$

where we have made use of the fact that $\exp(iK_{TE}\Lambda)$ - A_{TE} + B_{TE} = 0 at the quarter-wave condition. Next, we calculate the perturbed transfer matrix elements using Eq. (3),

$$\begin{aligned}\tilde{A}_{TE} &= A_{TE}+\Delta A_{TE}\\ &= e^{i(k_1+\Delta k_1)a}\left[\cos[(k_2+\Delta k_2)b]+\frac{i}{2}\left(\frac{k_2+\Delta k_2}{k_1+\Delta k_1}+\frac{k_1+\Delta k_1}{k_2+\Delta k_2}\right)\sin[(k_2+\Delta k_2)b]\right]\\ &\approx i(1+i\Delta k_1 a)\left[-\Delta k_2 b+\frac{i}{2}\left(\frac{k_2}{k_1}+\frac{k_1}{k_2}\right)\left(1+\frac{2k_2\Delta k_2+2k_1\Delta k_1}{k_2^2+k_1^2}-\frac{\Delta k_1}{k_1}-\frac{\Delta k_2}{k_2}\right)\right]\end{aligned} \quad (12)$$

resulting in a matrix element perturbation

$$\begin{aligned}\Delta A_{TE} = {} & \Delta k_1\left[\frac{1}{2k_1}\left(\frac{k_2}{k_1}+\frac{k_1}{k_2}\right)-\frac{1}{k_2}-i\left(\frac{\pi}{4k_1}\right)\left(\frac{k_2}{k_1}+\frac{k_1}{k_2}\right)\right]\\ & +\Delta k_2\left[\frac{1}{2k_2}\left(\frac{k_2}{k_1}+\frac{k_1}{k_2}\right)-\frac{1}{k_1}-i\left(\frac{\pi}{2k_2}\right)\right].\end{aligned} \quad (13)$$

A similar analysis gives

$$\begin{aligned}\Delta B_{TE} = {} & \Delta k_1\left[\frac{-1}{2k_1}\left(\frac{k_2}{k_1}-\frac{k_1}{k_2}\right)-\frac{1}{k_2}-i\left(\frac{\pi}{4k_1}\right)\left(\frac{k_2}{k_1}-\frac{k_1}{k_2}\right)\right]\\ & +\Delta k_2\left[\frac{-1}{2k_2}\left(\frac{k_2}{k_1}-\frac{k_1}{k_2}\right)+\frac{1}{k_1}\right].\end{aligned} \quad (14)$$

#68524 - $15.00 USD Received 27 February 2006; revised 17 April 2006; accepted 18 April 2006

The matrix eigenvalue now contains a perturbation term that is easily calculated as [20,21]

$$\Delta(e^{iK_{\mathrm{TE}}\Lambda}) = \left\langle u_{\mathrm{TE}}, \Xi_{\mathrm{TE}} u_{\mathrm{TE}} \right\rangle = \mathrm{Re}(\Delta A_{\mathrm{TE}} - \Delta B_{\mathrm{TE}}) \tag{15}$$

where Ξ_{TE} is a field transfer perturbation matrix defined analogously to Eq. (4) and u_{TE} is the normalized eigenvector of Eq. (4), equal to $(1/\sqrt{2})[\text{-}1\ 1]^{\mathrm{T}}$ [20]. Finally, using Eq. (9) and Eqs. (13)-(15), Eq. (11) reduces to the TE mode detuning equation

$$(\Delta k_{\mathrm{co}})_{\mathrm{TE}} = \alpha_{\mathrm{TE}}(\Delta k_1 + \Delta k_2)_{\mathrm{TE}}\,, \quad \alpha_{\mathrm{TE}} = \frac{\pi k_{\mathrm{co}}}{t_{\mathrm{co}}(k_2^2 - k_1^2)}\,. \tag{16}$$

The TM mode detuning equation follows a similar derivation, with

$$\begin{aligned}
(\Delta k_{\mathrm{co}})_{\mathrm{TM}}^{\mathrm{EVEN}} &= \alpha_{\mathrm{TM}}^{\mathrm{EVEN}}[(n_2/n_1)^2 \Delta k_1 + \Delta k_2]_{\mathrm{TM}}^{\mathrm{EVEN}}\,, \quad \alpha_{\mathrm{TM}}^{\mathrm{EVEN}} = \frac{\pi k_{\mathrm{co}} n_1^4 n_2^2}{n_{\mathrm{co}}^2 t_{\mathrm{co}}(n_1^4 k_2^2 - n_2^4 k_1^2)} \\
(\Delta k_{\mathrm{co}})_{\mathrm{TM}}^{\mathrm{ODD}} &= \alpha_{\mathrm{TM}}^{\mathrm{ODD}}[(n_1 k_2/n_2 k_1)^2 \Delta k_1 + \Delta k_2]_{\mathrm{TM}}^{\mathrm{ODD}}\,, \quad \alpha_{\mathrm{TM}}^{\mathrm{ODD}} = \frac{(n_{\mathrm{co}} n_2 k_1)^2}{(n_1^4 k_2^2 - n_2^4 k_1^2)}\,.
\end{aligned} \tag{17}$$

Equations (16) and (17) implicitly relate any perturbation in the transverse propagation vectors k_i to a change in effective index. We are now in a position to calculate first-order dispersion by expanding Eq. (1) to first order in $\Delta\omega$ about ω_0,

$$\tilde{k}_i = k_i + \Delta k_i \approx \left(\frac{\omega_0 + \Delta\omega}{c}\right)\left[(n_i + n_i'\Delta\omega)^2 - (n_{\mathrm{eff}} + n_{\mathrm{eff}}'\Delta\omega)^2\right]^{1/2} \tag{18}$$

where the primes denote differentiation with respect to ω at $\omega=\omega_0$. A Taylor expansion of the square root, keeping terms up to first order in $\Delta\omega$, results in

$$\tilde{k}_i \approx \left(\frac{\omega_0 + \Delta\omega}{c}\right)\left(n_i^2 - n_{\mathrm{eff}}^2\right)^{1/2}\left[1 + \frac{(n_i n_i' - n_{\mathrm{eff}} n_{\mathrm{eff}}')}{n_i^2 - n_{\mathrm{eff}}^2}\Delta\omega\right]. \tag{19}$$

Comparing Eq. (19) to Eq. (1), and eliminating the term proportional to $(\Delta\omega)^2$,

$$\Delta k_i \approx \frac{\Delta\omega}{c}(G_i - H_i n_{\mathrm{eff}}') \tag{20}$$

with

$$G_i = \left(n_i^2 - n_{\mathrm{eff}}^2\right)^{1/2}\left(1 + \frac{\omega_0 n_i n_i'}{n_i^2 - n_{\mathrm{eff}}^2}\right) \tag{21}$$

and

$$H_i = \frac{\omega_0 n_{\mathrm{eff}}}{\left(n_i^2 - n_{\mathrm{eff}}^2\right)^{1/2}}\,. \tag{22}$$

#68524 - $15.00 USD Received 27 February 2006; revised 17 April 2006; accepted 18 April 2006

Finally, substituting Eqs. (20)-(22) into Eqs. (16)-(17), we solve for the first-order dispersion

$$n'_{\text{eff}} = \begin{cases} \dfrac{G_{\text{co}} - \alpha_{\text{TE}}[G_1 + G_2]}{H_{\text{co}} - \alpha_{\text{TE}}[H_1 + H_2]}, & \text{(TE)} \\ \dfrac{G_{\text{co}} - \alpha_{\text{TM}}^{\text{EVEN}}[(n_2/n_1)^2 G_1 + G_2]}{H_{\text{co}} - \alpha_{\text{TM}}^{\text{EVEN}}[(n_2/n_1)^2 H_1 + H_2]}, & \text{(TM, EVEN)} \\ \dfrac{G_{\text{co}} - \alpha_{\text{TM}}^{\text{ODD}}[(n_1 k_2/n_2 k_1)^2 G_1 + G_2]}{H_{\text{co}} - \alpha_{\text{TM}}^{\text{ODD}}[(n_1 k_2/n_2 k_1)^2 H_1 + H_2]}, & \text{(TM, ODD)}. \end{cases} \tag{23}$$

For waveguides comprised of isotropic materials, polarization dependence in $\partial n_{\text{eff}}/\partial\omega$ arises entirely through the term α, due to the polarization independence of n_{eff} under the quarter-wave condition. Furthermore, it is clear that the birefringence Δn_{eff} of the QtW-BRW must change sign at the QtW wavelength;

$$\begin{aligned} \Delta n_{\text{eff}} &= n_{\text{eff,TE}} - n_{\text{eff,TM}} \\ &= \left[n_{\text{eff}} + \left(\frac{\partial n_{\text{eff}}}{\partial \omega} \right)_{\text{TE}} \Delta\omega \right] - \left[n_{\text{eff}} + \left(\frac{\partial n_{\text{eff}}}{\partial \omega} \right)_{\text{TM}} \Delta\omega \right] \\ &= \left[\left(\frac{\partial n_{\text{eff}}}{\partial \omega} \right)_{\text{TE}} - \left(\frac{\partial n_{\text{eff}}}{\partial \omega} \right)_{\text{TM}} \right] \Delta\omega . \end{aligned} \tag{24}$$

The terms $n_i', n_i'' \ldots$ are properties of the material system studied, and can be expressed analytically using appropriate semi-empirical Sellmeier coefficients or Adachi [22], Afromowitz [23], Pikhtin-Yas'kov [24], or Gehrsitz [25] formulae, for example. Alternatively, one can utilize a look-up table of experimental refractive index data [26], although data smoothing algorithms may be necessary for calculation of second- or higher-order dispersion due to the inherent problem of calculating high-order derivatives of noisy data. In the next section, we will discuss the effects of uncertainty in material dispersion on calculation of waveguide dispersion.

We now apply Eq. (23) to the analysis of an $Al_xGa_{1-x}As$ QtW-BRW operating at a nominal wavelength of 1.55 μm. To provide a strong resonance in the cladding, we utilize a very large index difference, $GaAs/Al_{.75}Ga_{.25}As$, with material indices calculated using [25]. The range of valid core indices and thicknesses in a QtW-BRW is determined by the requirement that the effective index is lower than all material indices. This ensures that the mode is not evanescent in any layer, a condition that would otherwise prevent the possibility of a $\pi/2$ phase thickness. As $n_1 > (n_{\text{co}}, n_2)$ by definition, this requirement dictates that $0 < n_{\text{eff}} < \min(n_{\text{co}}, n_2)$ [20], resulting in the constraints

$$\begin{aligned} &\frac{\pi c}{\omega_0 n_{\text{co}}} < t_{\text{co}} < \frac{\pi c}{\omega_0 \sqrt{n_{\text{co}}^2 - n_2^2}}, && (n_{\text{co}} > n_2) \\ &\frac{\pi c}{\omega_0 n_{\text{co}}} < t_{\text{co}}, && (n_{\text{co}} < n_2). \end{aligned} \tag{25}$$

We choose a core composition of $Al_{.90}Ga_{.10}As$ and a core thickness of 350 nm. Material dispersion data is shown in Table 1. By Eq. (8), this 1-D waveguide has a polarization-independent effective index of 1.9235 at 1.55 μm. Cladding layer thicknesses (required only

#68524 - $15.00 USD Received 27 February 2006; revised 17 April 2006; accepted 18 April 2006

to model the BRW at wavelengths that do not correspond to the quarter-wave condition) are determined by Eqs. (1) and (7). Figure 2 shows the effective index curves for this waveguide, obtained by solving Eq. (2) at each wavelength in a region around 1.55 μm. Note the change of sign for the birefringence, as predicted. Normalized first-order dispersion $\omega(\partial n_{\text{eff}}/\partial\omega)$ is shown in Fig. 3. The analytical solution at 1.55 μm obtained using Eq. (23) is plotted as well, showing complete agreement with the numerical curves.

Table 1. Material dispersion data for the waveguides analyzed in Figs. 2-3, 5-7, λ=1.55 μm (from [25])

Layer	Material	n_i	n_i' [x 10^{-16} s]	n_i'' [x 10^{-32} s^2]
Core	$Al_{0.9}Ga_{0.1}As$	2.933	0.067	5.588
Cladding 1	GaAs	3.374	1.345	14.993
Cladding 2	$Al_{0.75}Ga_{0.25}As$	3.000	0.074	6.432

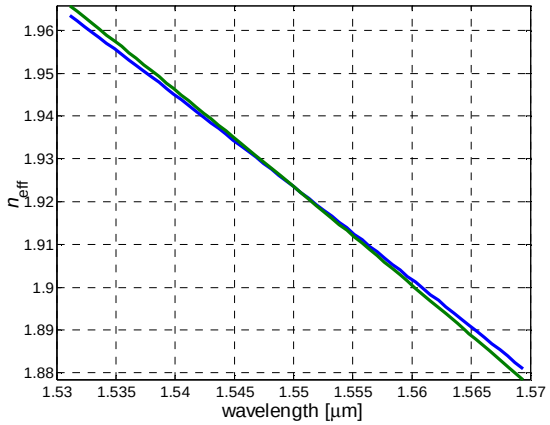

Fig. 2. Effective index for a BRW that is quarter-wave at 1.55 μm. (Blue: TE, green: TM).

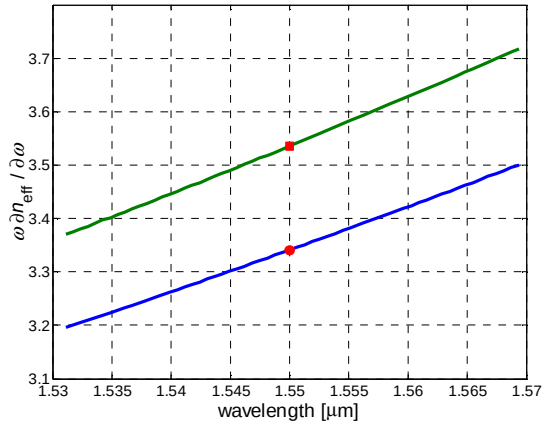

Fig. 3. Normalized first-order dispersion for the waveguide of Fig. 2. (Blue: TE, green: TM).
● Analytical solution from Eq. (23) (TE), ■ Analytical solution (TM).

#68524 - $15.00 USD Received 27 February 2006; revised 17 April 2006; accepted 18 April 2006

Second-order dispersion – or group velocity dispersion (GVD) – is derived analogously. Expanding Eq. (1) to second order about ω_0,

$$\tilde{k}_i \approx \left(\frac{\omega_0+\Delta\omega}{c}\right)\left[\left(n_i+n_i'\Delta\omega+\frac{1}{2}n_i''(\Delta\omega)^2\right)^2-\left(n_{\text{eff}}+n_{\text{eff}}'\Delta\omega+\frac{1}{2}n_{\text{eff}}''(\Delta\omega)^2\right)^2\right]^{1/2} \tag{26}$$

and a Taylor expansion of the square root, $(1+\gamma_1 x+\gamma_2 x^2)^{1/2} \approx 1+\gamma_1 x/2+(\gamma_2/2-\gamma_1^2/8)x^2$, keeping terms up to second order in $\Delta\omega$, gives

$$\tilde{k}_i \approx \left(\frac{\omega_0+\Delta\omega}{c}\right)(n_i^2-n_{\text{eff}}^2)^{1/2}\left[1+J_i\Delta\omega+P_i(\Delta\omega)^2-\frac{1}{2}\frac{n_{\text{eff}}n_{\text{eff}}''}{n_i^2-n_{\text{eff}}^2}(\Delta\omega)^2\right] \tag{27}$$

with

$$J_i=\frac{n_i n_i'-n_{\text{eff}}n_{\text{eff}}'}{n_i^2-n_{\text{eff}}^2} \tag{28}$$

and

$$P_i=\frac{1}{2}\left[\frac{n_i n_i''+(n_i')^2-(n_{\text{eff}}')^2}{n_i^2-n_{\text{eff}}^2}-\frac{(n_i n_i'-n_{\text{eff}}n_{\text{eff}}')^2}{(n_i^2-n_{\text{eff}}^2)^2}\right]. \tag{29}$$

Comparing Eq. (27) to Eq. (1), and eliminating the terms proportional to $(\Delta\omega)^3$,

$$\Delta k_i \approx \frac{\Delta\omega}{c}(G_i-H_i n_{\text{eff}}')+\frac{(\Delta\omega)^2}{c}(S_i-T_i n_{\text{eff}}'') \tag{30}$$

where

$$S_i=(n_i^2-n_{\text{eff}}^2)^{1/2}(J_i+\omega_0 P_i) \tag{31}$$

and

$$T_i=\frac{\omega_0 n_{\text{eff}}}{2(n_i^2-n_{\text{eff}}^2)^{1/2}}. \tag{32}$$

Finally, using Eqs. (16)-(17) and (30)-(32), we solve for the second-order dispersion, noting that the terms involving G_i and H_i cancel out due to Eq. (23):

$$n_{\text{eff}}''=\begin{cases}\dfrac{S_{\text{co}}-\alpha_{\text{TE}}[S_1+S_2]}{T_{\text{co}}-\alpha_{\text{TE}}[T_1+T_2]}, & \text{(TE)}\\ \dfrac{S_{\text{co}}-\alpha_{\text{TM}}^{\text{EVEN}}[(n_2/n_1)^2S_1+S_2]}{T_{\text{co}}-\alpha_{\text{TM}}^{\text{EVEN}}[(n_2/n_1)^2T_1+T_2]}, & \text{(TM, EVEN)}\\ \dfrac{S_{\text{co}}-\alpha_{\text{TM}}^{\text{ODD}}[(n_1k_2/n_2k_1)^2S_1+S_2]}{T_{\text{co}}-\alpha_{\text{TM}}^{\text{ODD}}[(n_1k_2/n_2k_1)^2T_1+T_2]}, & \text{(TM, ODD)}.\end{cases} \tag{33}$$

#68524 - $15.00 USD Received 27 February 2006; revised 17 April 2006; accepted 18 April 2006

In contrast to the first-order dispersion shown in Eq. (23), the polarization dependence of GVD arises not only due to the α terms, but also to the S_i terms, via J_i and P_i, which reflect the polarization dependence of first-order dispersion. In general, nth-order dispersion can be calculated in a similar iterative fashion by keeping terms up to order $(\Delta\omega)^n$ in the expansion of Eq. (1) and applying the results of all lower orders, although the resulting accuracy diminishes due to the use of successive lower-order approximations. The analytical solutions are strictly valid at the nominal (quarter-wave) frequency. When calculating the effective index in a region around this frequency, the bandwidth over which these dispersion figures are valid is dependent upon the particular design – it can be estimated by calculating the next-lowest order of dispersion. For this reason, choosing a nominal operating wavelength far from the material bandgap will result in an extended bandwidth. An example is given in [20] for first-order dispersion.

4. Discussion

As with all waveguides, the dispersion of a QtW-BRW is dependent on both the material and geometry. Separating these components in Eqs. (23) and (33) is difficult, but it is instructive to examine the case where the material dispersion can be considered negligible, for example in III-V semiconductors with photon energies far below the bandgap. This study is motivated by the significant discrepancy among various III-V dispersion models in the literature (e.g. [22-25]). Figure 4 shows compositional dependence of refractive index and index dispersion for $Al_xGa_{1-x}As$ at 1.55 μm using three of these models. Here and throughout this work, we describe second-order dispersion using the dispersion parameter $\beta_2 \equiv \partial^2\beta/\partial\omega^2 = (\omega/c)\partial^2 n/\partial\omega^2 + (2/c)\partial n/\partial\omega$. While there is close agreement between the models of Afromowitz and Gehrsitz, the model of Adachi differs significantly, especially for low aluminum fraction. It should be noted that in this wavelength region, the latter model relies on an extrapolation of empirical data from photon energies closer to the bandgap for $0 \le x \le 0.38$, and additional data from the same source as used by Afromowitz at x = 1 in the mid-IR; this is a possible source of the discrepancy. The uncertainty in material dispersion will lead to inaccuracies in calculating dispersion of the QtW-BRW; however, comparing the magnitudes of the quantities plotted in Figs. 3 and 4(b), it is clear that for this particular waveguide, material dispersion plays a relatively small role, which is more than one order of magnitude less than that of the waveguide dispersion.

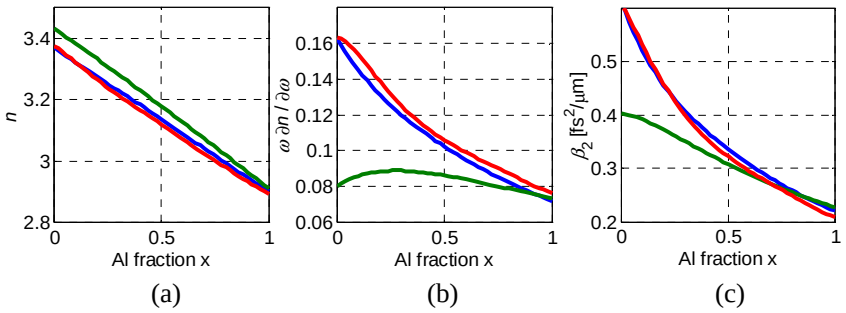

Fig. 4. Index dispersion of $Al_xGa_{1-x}As$ at 1.55 μm using three different models. (a) refractive index (b) normalized first-order dispersion (c) second-order dispersion parameter β_2. Blue: Afromowitz [23], Green: Adachi [22], Red: Gehrsitz *et al.* [25].

Here, we examine the calculation of total dispersion under the assumption that material dispersion is zero. The test structure has the same composition as the waveguide analyzed in Figs. 2-3, but the core thickness is allowed to vary in order to produce an effective index between 0 and n_{co}. Cladding layer thicknesses are altered accordingly to maintain QtW operation by Eqs. (1) and (7). We define a normalized effective index *B*, which bears some resemblance to the normalized propagation constant used in the analysis of total internal

#68524 - $15.00 USD Received 27 February 2006; revised 17 April 2006; accepted 18 April 2006

reflection waveguides; the variation of B with t_{co} for waveguides of this composition is shown in Fig. 5:

$$B \equiv \frac{n_{\text{eff}}}{n_{\text{co}}} = \sqrt{1 - \left(\frac{\pi c}{\omega_0 t_{\text{co}} n_{\text{co}}} \right)^2} \quad . \tag{34}$$

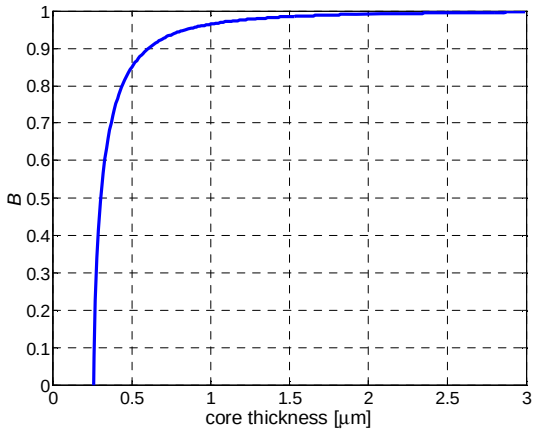

Fig. 5. Normalized effective index vs. core thickness for various QtW-BRWs with core and cladding compositions identical to the waveguide analyzed in Figs. 2 and 3.

The normalized effective index is critically related to the dispersion. From Eqs. (16)-(23), it is apparent that in the limit $B \rightarrow 0$, $G_i \rightarrow n_i + \omega_0 \partial n_i/\partial\omega$, $H_i \rightarrow 0$, and thus $\partial n_{\text{eff}}/\partial\omega \rightarrow \infty$ (first-order pole) for both TE and TM, regardless of the magnitude of material dispersion. Similarly, $\partial^2 n_{\text{eff}}/\partial\omega^2 \rightarrow -\infty$ (second-order pole). We shall denote this as the "waveguide dispersion" limit, where the material dispersion is negligible. Operating near this point offers the possibility of ultra-slow light propagation due to the large group index, $N_g = n_{\text{eff}} + \omega(\partial n_{\text{eff}}/\partial\omega)$, with large anomalous GVD. From Fig. 5, it appears that the tolerance of B to minor variations in core thickness is extremely tight. This issue can be compensated for by designing the BRW as a *p-i-n* structure, with the core as an intrinsic layer, then tuning the resonance by carrier injection as described in [2,27].

In the "material dispersion" limit $B \rightarrow 1$, the term $\alpha \rightarrow 0$, and thus $\partial n_{\text{eff}}/\partial\omega$ approaches $\partial n_{\text{co}}/\partial\omega$ and $\partial^2 n_{\text{eff}}/\partial\omega^2 \rightarrow \partial^2 n_{\text{co}}/\partial\omega^2$. This represents the situation where all power is confined within the core, with the physically unrealizable requirement of infinite core thickness. In this regime, the assumption of negligible material dispersion is invalid and will lead to relatively significant errors in estimating dispersion. An interesting result of this analysis of the limiting cases is that if the core material has normal GVD, there exists a waveguide design that will provide zero GVD, and a very wide range of core thicknesses that provide the low GVD desired for soliton formation.

In Fig. 6, the normalized first-order dispersion is plotted over the range $0.01 < B < 0.999$, with and without the contribution of material dispersion. There is negligible difference for $B < 0.9$, suggesting that accurate values of material dispersion are not required in this range. As expected, the normalized dispersion approaches $\omega(\partial n_{\text{co}}/\partial\omega) \approx .081$ as $B \rightarrow 1$ [see Fig. 4(b)]. Only the TE mode is considered here; the TM mode exhibits similar characteristics. The GVD parameter $-\beta_2$ is plotted in Fig. 7 (using the negative dispersion parameter has no physical significance; it only allows the logarithmic scale to be used). The inset shows the region around $B \approx 1$, where β_2 approaches the core value of 0.23 fs^2/μm [see Fig. 4(c)] As mentioned previously, there is a waveguide design for which $\beta_2 = 0$, at $B \approx 0.996$, or by Fig. 5, $t_{\text{co}} \approx 3$ μm.

#68524 - $15.00 USD Received 27 February 2006; revised 17 April 2006; accepted 18 April 2006

The small variation of B with t_{co} in this range suggests that thickness tolerance is not an issue. Furthermore, the wide core need not be an impediment to single-mode operation, as guided modes in BRWs need to satisfy both the resonance condition in the core and the Bragg condition in the cladding [18].

It can also be shown that for the TE and even TM mode, normal first-order material dispersion implies normal first-order waveguide dispersion. Using Eqs. (16), (17), (21), and (22), and recalling that $n_{eff} < n_i$, it is clear that G_i and H_i are positive quantities and α_{TE}, α_{TM}^{EVEN} are negative. Thus, by Eq. (23), $\partial n_{eff}/\partial\omega > 0$ for all values of B.

From the above examples, we can see that the use of analytical formulae, Eqs. (23) and (33), has greatly facilitated the analysis of QtW-BRWs. The method presented here serves as a quick check for the existence of a zero-GVD wavelength for a given waveguide design. It also affords the ability to directly assess the effect of various BRW design parameters on the position of the zero-GVD wavelength. The analytical formulae developed here can also be used as a stepping stone for the study of higher order dispersion terms which are important for pulses with temporal widths in the femtosecond regime by a similarly rigorous analytical approach. The formulae also minimize the numerical errors encountered in purely numerical approaches, leaving the error limitations to those inherent to the material dispersion models. These errors are important in dispersion calculations because many devices operate in regimes around zero dispersion, where absolute errors are critical and where higher order terms are of substantial importance.

The implications for nonlinear optical propagation can be best highlighted by recalling that the threshold power for first-order solitons is proportional to β_2 and inversely proportional to the square of the pulse width [8]. This suggests an onset for soliton-like propagation within a BRW that is essentially controllable via the BRW parameters as seen in Fig. 7. This control over dispersion can take place also post waveguide growth. We have shown previously the capability of tuning the properties of BRWs using electro-optic as well as current injection effects [2, 27]. It is therefore evident that BRWs offer a practical tool for implementing nonlinear devices in compound semiconductors using low optical power for all-optical switching, for example.

In addition, the inset of Fig 7 demonstrates the capability of designing BRWs with a positive β_2. Note that this change in sign has been achieved solely through the waveguide dispersion control and does not include any excessive absorption due to a material resonance. This offers the capability of observing dark solitons in materials with self-focusing third-order nonlinearity using a low loss, tunable device [8], an attractive capability for optical switching and all-optical control devices.

5. Conclusion

Using a perturbation of the mode dispersion equation, formulae for first- and second-order dispersion of a quarter-wave Bragg reflection waveguide have been derived. Although the effective index of the BRW is polarization-independent at the quarter-wave point, the dispersion is not, and thus the sign of birefringence changes here. Furthermore, the first-order dispersion of symmetric fundamental modes is normal for waveguides composed of materials with normal dispersion. Depending on the design of the QtW-BRW, dispersion can be dominated by the core material (for large t_{co}) or by the waveguide form (for very narrow cores). In the latter regime, first-order and second-order dispersion asymptotically approach ∞ and $-\infty$ respectively, as the effective index approaches zero. Between these extreme limits, there exists a waveguide design that shows zero GVD. Due to the low loss nature of BRWs, as they do not possess refractive index modulation in the direction of propagation, they offer an attractive building block for nonlinear optics in semiconductors.

#68524 - $15.00 USD Received 27 February 2006; revised 17 April 2006; accepted 18 April 2006

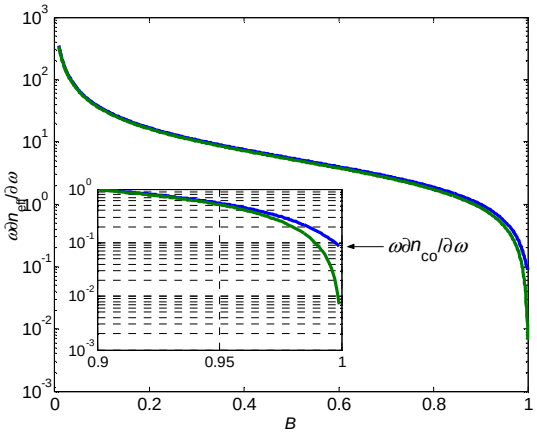

Fig. 6. Normalized first-order dispersion vs. normalized effective index of the TE mode including (blue) and omitting (green) the contribution of material dispersion. Inset: region around $B \approx 1$. The curves are indistinguishable for $B < 0.9$.

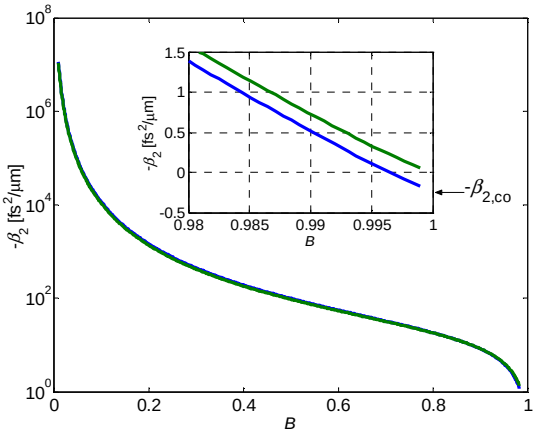

Fig. 7. Second-order dispersion parameter $-\beta_2$ vs. normalized effective index of the TE mode including (blue) and omitting (green) the contribution of material dispersion. Inset: region around $B \approx 1$ (linear scale). Negative β_2 is shown here only to facilitate the use of the logarithmic scale.

Acknowledgments

The authors wish to thank Sean Wagner for contributing to the AlGaAs dispersion modeling.

#68524 - $15.00 USD Received 27 February 2006; revised 17 April 2006; accepted 18 April 2006